22.0 FORMATION, HIGH TEMPERATURE STABILTIY, AND MECHANICAL PROPERTIES OF MICROEUTECTICS IN BULK SOLIDIFIED AL-FE-V-SI AND RELATED ALLOYS

Joe Jankowski (CSM)
Faculty: Michael Kaufman (CSM), Amy Clarke (CSM), Robert Field (CSM), and Steve Midson (CSM)
Industrial Mentor: Krish Krishnamurthy (Honeywell) and Paul Wilson (Boeing)

22.1 Project Overview and Industrial Relevance

The purpose of this project is to develop a high-performance structural aluminum alloy with acceptable high temperature strength through the formation of a lamellar microeutectic microstructure composed of aluminum and the cubic intermetallic phase α-$Al_{13}(Fe,V)_3Si$. The reason this alloy is of particular interest is that this microstructure can be formed at cooling rates of 10^2 to 10^3 K/s, which is orders of magnitude lower than rapid solidification (RS) cooling rates. This suggests this alloy system could represent a lower cost alternative to current high-temperature aluminum alloys produced by rapid solidification (e.g., RS8009), or by related methods such as powder metallurgy. The development of a lower cost aluminum alloy with acceptable high temperature mechanical properties would allow for improvements in part performance in industries where current RS alloys are prohibitively expensive.

In order to develop an alloy system that has a favorable microstructure, it is critical to minimize or prevent the formation of unwanted phases. In the case of the AlFeVSi system, a potentially deleterious phase may form that is of primary concern—the hexagonal $Al_{12.8}(Fe,V)_3Si_{0.3}$ phase (h-phase) with similar composition and a crystal structure related to the $Al_{13}(Fe,V)_3Si$ α-phase, but with a coarse dendritic morphology. Additionally, due to the high content of Fe in the baseline 8009 alloy, large $Al_{13}Fe_4$ (θ-phase) particles may form in sections on the order of 1cm in diameter in chill castings. It is therefore essential that mitigation strategies promote α-phase, while removing h-phase and θ-phase. To this end, concepts from physics/chemistry will be used to identify the workable composition space and will be supplemented by density functional theory (DFT) calculations and data from the literature.

The detailed characterization of the h-phase and incorporation of electronic structure information can not only be used to promote the microeutectic between $Al_{13}(Fe,V)_3Si$ and aluminum, but may also provide information about how to improve existing RS alloys and develop new alloys optimized for additive manufacturing. Commercial RS8009 alloys are known to contain the h-phase, which is typically coarser than the desired dispersion of α-$Al_{13}(Fe,V)_3Si$ [22.1]. The use of conceptual tools from chemistry and physics, coupled with DFT, should allow for the rapid optimization of microeutectic volume fraction in a huge composition space. The methodology used in this work will be applicable to essentially all Al-TM (transition metal) and Al-TM-Si alloys.

22.2 Previous Work

Several important findings were made prior to this reporting period. First, the as-cast microeutectic structure was found to have hardness values comparable to extruded RS8009 and stable at temperatures well above potential operating temperatures (250 to 300 °C). The thermal stability and high hardness of the microeutectic were two of the initial findings that suggested its potential. Since high hardness alone is not sufficiently indicative of desirable mechanical properties, a three-point bending test was performed on a sample that contained a significant volume fraction of the microeutectic structure. The fracture surface was indicative of ductile fracture. The high hardness, thermal stability, and ductility of the microeutectic indicate that if it can be produced throughout a cast part, it would likely exhibit desirable mechanical properties.

Another important result was the development of a detailed crystal structure model for the h-phase using synchrotron and neutron powder diffraction at U.S. DOE user facilities, coupled with charge flipping [22.2]. Based on this model, minor alloying additions of Co and Mn, and major alloying additions of Si were examined and were found to be beneficial for removing the h-phase, where the Si additions were especially effective. DFT calculations on the $Pm\bar{3}$ variant of the AlMnSi α-phase were used to determine workable compositions for the α-phase in Al alloys. It was found that V, Cr, Mo, Mn, and Fe were effective in stabilizing the α-phase and compositional rules for incorporating them were developed. Small additions of B were found to sometimes promote α-phase particle nucleation in the melt.

22.3 Recent Progress

Since the last CANFSA meeting, the main development has been developing a plan of work for the rest of the project. However, some experimental progress has been made on the project as well.

Limited TEM work was performed in order to determine the crystal structure of intermetallics in Al-Fe-Mn-Cr-Si castings designed to promote Al and α-phase. The intermetallics were identified to be either $Pm\bar{3}$ [22.3] or $Im\bar{3}$ [22.4] variants of the α-phase. It had been hypothesized that these two variants might have different solidification behavior, but no evidence was found to support that hypothesis. In addition, differential scanning calorimetry (DSC) was performed to determine the liquidus temperature of two Al-Fe-Mn-Cr-Si alloys and to assess the success of the present alloying strategy for reducing the liquidus temperature. A cooling rate analysis and repeatability study has been initiated with results that support the prior claims of cooling rates achieved in the copper chill molds used in this work.

Finally, experience in the maximum entropy method (MEM) / Rietveld analysis of extracting charge density [22.5] from experimental data was developed by performing an analysis of the metastable monoclinic phase in Al-Ge and the α-phase in Al-(Fe,Mn)-Si alloys. In combination with recent work demonstrating capabilities of producing relatively pure samples of α-phase at compositions relative to this project, this will set the stage for definitive crystallographic and DFT work on the α-phase.

22.3.1 TEM analysis of intermetallic particles

Unlike many conventional eutectic alloys, the Al + α-phase eutectic system does not exist in a well-defined compositional space. The α-phase can exist with many different compositions of the form $Al_{(83-x)}$-$(Fe,Mn)_{(17-y)}$-$(Mn,Cr,V,Mo)_y$-Si_x, although this form of describing the composition excludes some elements known to have significant solubility in the α-phase. The TEM work was performed to assess whether or not minor changes in crystal structure occurred with changes in composition and whether such changes had any effect on the solidification behavior in these Al-Fe-Mn-Cr-Si alloys. It was found that, while compositional and structural differences exist between different morphologies of the α-phase, these differences are what would be expected given the solidification sequence in the alloys. As such, there was no evidence that this line of work was worth investigating further.

22.3.2 DSC analysis of liquidus temperatures

DFT work performed in the previous reporting period was able to develop rough compositional rules for α-phase formation. As a result, alloys likely to produce only Al and α-phase at the cooling rates in question can be easily identified. With this knowledge, the question was not what compositions can produce the microeutectic, but which compositions that can produce the microeutectic have the best properties? To retain the coarsening resistance of 8009, an appreciable level of elements with low diffusivity and solubility in Al is required. For the purposes of this project, only Cr and V will be considered due to their favorable phase diagrams with Al (relative to refractory metals). With the constraint that a certain level of Cr or V needs to be included, the equilibrium liquidus seemed to be a good target for optimization given that 100 K of superheat above the eutectic is approximately equal to 25% more heat that needs to be extracted prior to full solidification. This leads to longer solidification times and lower cooling rates (and by extension lower undercoolings). In 8009, the estimated superheat above the eutectic temperature for casting into the chill mold is about 300-400 K. This is exceedingly high and contributes substantially to difficulties in producing fully eutectic alloys as the heat removed due to the superheat is on the same order of magnitude as the heat removed due to solidification. An Al-Fe-Mn-Cr-Si alloy with comparable overall transition metal content compared to 8009 had an equilibrium liquidus temperature about 75 K lower. This is attributed to the formation of α-phase as the primary phase instead of the θ-phase, as predicted by Thermo-Calc. Lower equilibrium liquidus temperatures help with achieving the undercoolings necessary to form the α-phase in the eutectic morphology instead of coarse primary particles.

22.3.3 Cooling Rate Analysis and Repeatability

The most recent work performed this reporting period has been the experimental determination of cooling rates in the stepped cylindrical copper chill mold as a function of distance from the mold wall for the different section diameters, namely the 6 mm and 8 mm diameters. It was found that for the 2 mm through 8 mm diameter sections, a maximum cooling rate approaching 10^4 K/s was achieved near the mold wall for 2 mm and a minimum cooling rate around 200 K/s was achieved in the center of the 8mm diameter casting. Broadly speaking, for the 6mm and 8mm diameter castings, cooling rates were between about 200 K/s and about 1,000 K/s. The reference material for cooling rate measurements was 356 cast with a superheat of 100 K (720 °C) as measured by a type K thermocouple immediately prior to casting. The secondary dendrite arm spacing (SDAS) was measured in the castings to

determine the cooling rate experienced during solidification [6]. The recorded values as a function of distance from the mold wall are shown in **Fig. 22.1**. In addition to measuring the cooling rate, special attention was paid to the range of cooling rates at different distances from the mold wall in order to understand the range of solidification conditions that can occur as a function of distance from the mold wall. Initial results were relatively promising, with a relatively low spread in the cooling rates for a given distance away from the mold wall.

22.3.4 Proposed Work for Project

Much of the work for the past reporting period has been the development of a detailed plan of work for the remainder of the project. As such, the plans will be outlined in this report.

The first part of the work is the development of a detailed crystallographic model of the α-phase as a function of composition. Sufficient work in this area has not yet been done to allow for DFT calculations to perform quantitative or even qualitative prediction of α-phase compositions for all elements (especially Si). Part of the reason for the lack of work has been the difficulty in making samples of α-Al-(Fe,V)-Si and α-Al-(Fe,Cr)-Si and to a certain extent lack of knowledge on the real extent of compositions over which the phase can form. Recently, samples have been prepared of different Al-(Fe,Mn)-Si, Al-(Fe,V)-Si, and Al-(Fe,Cr)-Si alloys with 3 compositions of the α-phase for each quaternary system. The combination of detailed compositional information from wavelength dispersive spectroscopy (WDS) and detailed crystallographic information from MEM/Rietveld analysis (using lab data shown in **Fig. 22.2**) on synchrotron powder diffraction data should yield unprecedented information on the α-phase over a broad composition range (as opposed to the Al-Fe-Mn-Si system alone). This will allow for DFT calculations that properly account for all elements in the α-phase and enable high accuracy *ab initio* composition predictions.

The second part is the development of a microstructure-cooling rate-composition diagram for either the Al-Fe-Mn-Cr-Si or Al-Fe-Mn-V-Si alloy system. This will build on the cooling rate / repeatability study for both the actual cooling rates associated with microstructures and the uncertainty associated with the cooling rate.

The third part is the study of fundamental solidification behavior in the quinary system chosen for the previous study by performing autogenous TIG welding with controlled weld speed and power to determine the link between solidification velocity, thermal gradients, cooling rates, and final microstructure. The experimental work will be supported by simulations using SYSWELD or another finite element method (FEM) software package for a weld on a plate. TIG welding was chosen since cooling rates in thin plates can be tuned in the 100 K/s to 1000 K/s range fairly easily with controlled solidification velocities.

The last solidification study will be to further clarify the effects of B additions on primary α-phase particle formation. In Cr, V, and Mo-containing samples, B additions have been observed to promote nucleation of α-phase particles. The mechanism and extent to which this behavior is controlled is unknown. The study will seek to clarify the compositions where B is effective and what the likely mechanism is using a combination of SEM and TEM analysis. For highly processing-sensitive compositions, this could prove important in making them commercially viable.

Finally, mechanical testing will be performed on promising alloys if high quality samples can be produced. This will either be done through hardness, compression, or tensile testing depending on the geometry of the samples produced.

22.4 Plans for Next Reporting Period

The future work for the project has been described, but the planned work for the next reporting period is as follows:

- Finish repeatability and cooling rate study
- Determine final quinary alloy system and characterize liquidus temperatures
- Develop general α-phase crystal structure and begin DFT calculations for predicting α-phase composition
- Begin work on composition-cooling rate-microstructure diagram

22.5 References

[1] Marshall, R. (2015). Master's Thesis.
[2] Baerlocher, C., McCusker, L. B. & Palatinus, L. (2007). *Z. Kristallogr.* 222, 47–53.

[3] Cooper, M. (1966). *Acta Crystallographica* 20, 614-617.
[4] Cooper, M. (1967). *Acta Crystallographica* 23, 1106-1107.
[5] Momma, K. *et al*. (2013). *Powder Diffraction* 28, 184-193.
[6] Wang, Q.G., Apelian, D., and Lados, D.A. (2001). *Journal of Light Metals*, 85-97.

22.6 Figures and Tables

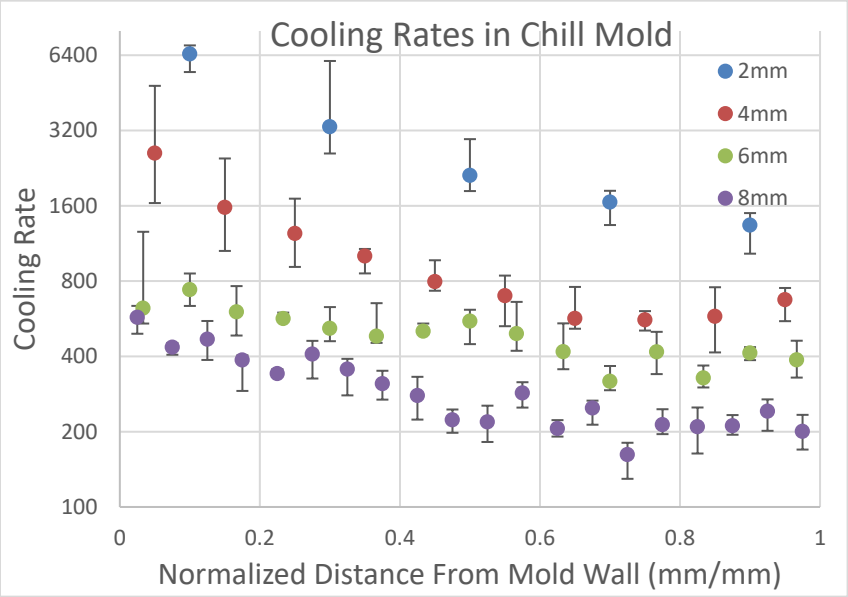

Figure 22.1: Cooling rate as measured by SDAS in 356 cast into the stepped cylindrical Cu chill mold. Normalized distance from mold wall is shown such that 0 is at the mold wall and 1 is at the center of the casting. Data points shown are the median and the error bars represent the first and third quartiles. Each point represents a distribution of 40 measurements. Error bars typically decrease as distance from mold wall increases, reflecting local variability in the heat transfer coefficient. The measured cooling rate is likely below the actual cooling rate due to sectioning effects when measuring dendrite arm spacing.

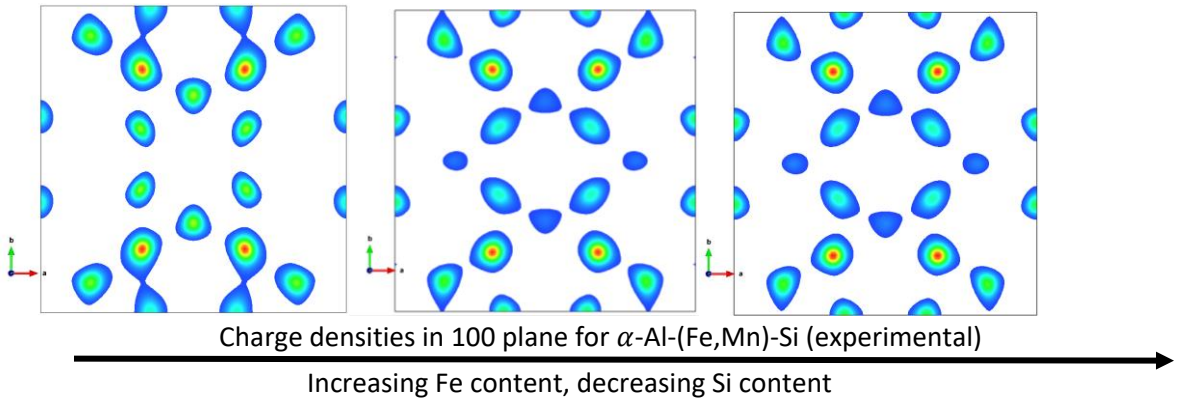

Figure 22.2: Isosurfaces of the charge density from lab diffraction data showing changes in structure in α-phase as a function of composition. Synchrotron data is expected to give much higher charge density and spatial resolution. The charge density on the left is from α-AlMnSi and the two on the right are from different compositions of α-Al(Fe,Mn)Si. Nuclear positions and bonding information are visible in the charge density.